12 Feb 87

Earth and Planetary Science Letters, 53 (1981) 189–202
Elsevier Scientific Publishing Company, Amsterdam – Printed in The Netherlands

[6]

TRACE ELEMENT AND ISOTOPIC EFFECTS OF COMBINED WALLROCK ASSIMILATION AND FRACTIONAL CRYSTALLIZATION

DONALD J. DePAOLO

Department of Earth and Space Sciences, University of California, Los Angeles, CA 90024 (U.S.A.)

Received June 27, 1980
Revised version received January 8, 1981

Equations describing trace element and isotopic evolution in a magma chamber affected simultaneously by fractional crystallization and wallrock assimilation are presented for a model where the mass assimilation rate ($\dot{M}_a$) is an arbitrary fraction (r) of the fractional crystallization rate ($\dot{M}_c$). The equations also apply to recharge of a crystallizing magma. Relatively simple analytical expressions are obtained for both radiogenic isotope variations (Nd, Sr, Pb) and stable isotopes (O, H) including the effects of mass-dependent fractionation. For $r = 1$ a modified zone refining equation is obtained for trace element concentrations, but for $r < 1$ behavior is a combination of zone refining and fractional crystallization. As $r \to \infty$, simple binary mixing is approached. The isotopic and trace element "mixing" trends generated can be much different from binary mixing, especially for $r < 1$. The model provides the basis for a more general approach to the problem of wallrock assimilation, and shows that binary mixing models are insufficient to rule out crustal assimilation as a cause of some of the isotopic variations observed in igneous rocks, including cases where clustering of isotopic values occurs partway between presumed endmember values. The coupled assimilation-fractional crystallization model provides an explanation for certain trace element and isotopic properties of continental margin orogenic magmas (e.g. Sr concentration versus $^{87}Sr/^{86}Sr$) which had previously been interpreted as evidence against assimilation. So-called "pseudoisochrons" can be understood as artifacts of contamination using this model. A significant correlation exists between country rock age and low $^{143}Nd/^{144}Nd$ ratios in continental igneous rocks, clearly suggestive that crustal contamination is generally important.

1. Introduction

The formation of igneous rocks has generally been conceptualized in terms of discrete and relatively simple constructs which idealize stages in the generation and evolution of magma. These constructs have tended to govern the interpretation of trace element patterns and isotopic properties of igneous rocks [1–4] even though they may be only rough approximations to the processes operating.

Recently the fundamentally continuous nature of magmatic petrogenesis has been emphasized by Carmichael et al. [5]. With regard to trace elements O'Hara et al. [6] and Langmuir et al. [7] have shown that consideration of more complex models for magma evolution, which plausibly represent particular physical situations, may lead to conclusions which are much different from those which would result from only consideration of zeroeth-order models, such as batch partial melting, fractional crystallization, or simple two-component mixing. Allègre and Minster [8] summarized a large number of models that could be applicable to igneous petrogenesis, but these models have not yet been generally applied.

A problem of particular concern which will be addressed here is the extent to which magmas are modified during ascent and emplacement, an understanding of which is critical if the rocks are to be used to infer properties of the magma source. This problem has been discussed at length by Bowen [9] and recently by Taylor [10] with regard to wallrock assimilation and fractional crystallization. Both authors point out that although these processes are often

0012-821X/81/0000–0000/$02.50

treated separately, heat-balance considerations suggest that the two should be coupled. Heat required for assimilation can be provided by the latent heat of crystallization of the magma. Barker et al. [11] presented petrologic evidence for the concurrent operation of these processes in the generation of the Pikes Peak batholith. Taylor calculated the effects of concurrent assimilation and fractional crystallization on the strontium and oxygen isotopic composition of a magma, and showed that the resulting effects are significantly different from those predicted by simple two-endmember mixing models. The results were presented in graphical form; the details of the calculations were not given. An equation describing trace element behavior for this type of process has been presented by Allègre and Minster [8].

It is the purpose of this paper to present the equations describing both isotopic effects and trace element effects for a general model of concurrent assimilation and fractional crystallization, since this approach shows potential for broadening the basis of discussion of this fundamental problem. This represents an amplification, with some modifications, of one model within the general approach discussed by Allègre and Minster [8]. Implications for the interpretation of trace element and isotopic patterns are then explored.

2. Assimilation-fractional crystallization (AFC) equations

2.1. Elemental concentrations

Consider a magma body (Fig. 1) of mass M_m which is assimilating wallrock at a rate $\dot{M}_a$ (mass/unit time) and crystallizing, with $\dot{M}_c$ representing the rate at which fractionating phases are being effectively separated from the magma. The magma here could be thought of as silicate liquid plus possibly entrained neutrally-buoyant crystals which do not separate from the liquid. The instantaneous rate of change of the mass (μ) of an element in the magma is given by:

$$\frac{d\mu}{dt} = \dot{M}_a C_a - \dot{M}_c D C_m = C_m \frac{dM_m}{dt} + M_m \frac{dC_m}{dt} \qquad (1a)$$

which can be rearranged to give:

$$\frac{dC_m}{dt} = \frac{\dot{M}_a}{M_m}(C_a - C_m) - \frac{\dot{M}_c}{M_m}(D - 1)C_m \qquad (1b)$$

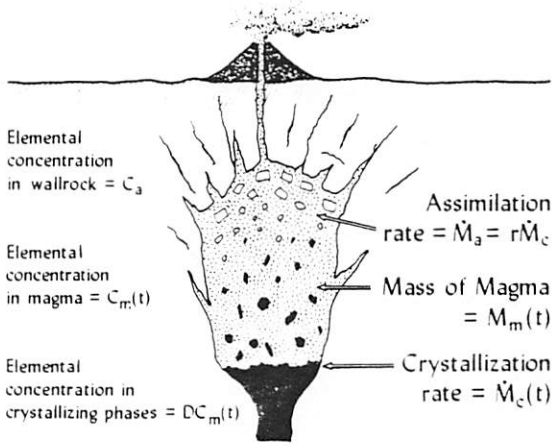

Fig. 1. Model for assimilation and fractional crystallization in a magma chamber.

where C_m is the concentration of the element in the magma ($= \mu/M_m$), C_a is the concentration of the element in the assimilated wallrock, D is the bulk solid/liquid partition coefficient for the element between the fractionating crystalline phases and the magma.

The solutions to this equation can be conveniently separated into two cases, one for $\dot{M}_a = \dot{M}_c$ and the other for $\dot{M}_a \neq \dot{M}_c$. For the former, (1b) reduces to:

$$\frac{dC_m}{dt} = \frac{\dot{M}_a}{M_m}(C_a - DC_m) \qquad (2)$$

which is analogous to zone refining [12].

For this case the material assimilated is balanced by an equivalent mass of material fractionated, so the mass of the magma is constant. Although this case may not apply over any large fraction of the history of a magma body, this simple differential equation exhibits the fundamental difference between the combined crystallization-assimilation case and the simple binary mixing model [7,13] which can be obtained by setting $\dot{M}_c = 0$ in (1). This difference is that the change in concentration in the residual magma is dependent not on the concentration difference between magma and wallrock, but on the concentration difference between the wallrock and the cumulates. Even if C_a is less than C_m, C_m can increase if $D < C_a/C_m$ and vice versa. Therefore, the tenet of the simple mixing model, that the concentration in the magma will change in the direction of that in the wallrock [13] is not necessarily true if fractional crystallization is also operating. Integration of (2) for

D and C_a constant leads to:

$$C_m/C_m^0 = (C_a/DC_m^0)[1 - \exp(-DM_a/M_m)] + \exp(-DM_a/M_m) \quad (3)$$

where C_m^0 is the original concentration in the magma and $M_a = \int_0^t \dot{M}_a \, d\tau$ is the total mass of material assimilated (≡ total mass fractionated).

In general, $M_a \neq M_c$. A more useful model which is soluble in closed form is obtained for a constant value of the ratio $r = \dot{M}_a/\dot{M}_c$. For this case (1b) can be written:

$$\frac{dC_m}{d \ln F} = \frac{r}{r-1} C_a - zC_m \quad (4)$$

where:

$$z = \frac{r + D - 1}{r - 1}$$

$$F = M_m/M_m^0$$

M_m^0 = initial mass of magma.

The variable has been changed from t to F using:

$$d \ln F = dM_m/M_m = M_m^{-1}(\dot{M}_a - \dot{M}_c)\, dt = M_m^{-1}(r-1)\dot{M}_c \, dt \quad (5)$$

This transformation is not applicable for $r = 1$. Integration of (4) results in:

$$C_m/C_m^0 = F^{-z} + \left(\frac{r}{r-1}\right)\frac{C_a}{zC_m^0}(1 - F^{-z}) \quad (6a)$$

Note that if $r + D = 1$, then $z = 0$. As $z \to 0$, $F^{-z} \to 1 - z \ln F$. Therefore, for this special case the result is:

$$C_m/C_m^0 = 1 + \left(\frac{r}{r-1}\right)\frac{C_a}{C_m^0} \ln F \quad (6b)$$

Returning to the case of constant magma mass ($\dot{M}_c = \dot{M}_a$), for $D \ll 1$ equation (3) reduces to:

$$C_m/C_m^0 = 1 + M_a C_a/M_m C_m^0 \quad (7)$$

For the case $D \gg 1$, (3) rapidly converges to:

$$C_m \approx C_a/D \quad (8)$$

when DM_a/M_m becomes large. This is in fact the limiting value for all values of D. For the more general case of changing magma mass, when $D \ll 1$ equation (6a) will reduce to the following form as F becomes small:

$$C_m/C_m^0 \approx F^{-1}\left[1 - \frac{C_a}{C_m^0}\frac{r}{(r-1)}\right] \quad (9)$$

This can be compared to the pure fractional crystallization case ($r = 0$) which is described by $C_m/C_m^0 = F^{-1}$ [1,2]. When D is large and $r < 1$, z is a large negative number and F^{-z} becomes small rapidly as F decreases. When $F^{-z} \ll 1$ equation (6a) becomes:

$$C_m \approx \frac{rC_a}{r + D - 1} \quad (10)$$

Fig. 2 shows the relationship between F and the relative concentration of an element for $r = 0.2$ and several values of D and C_a/C_m^0.

Compared to simple fractional crystallization (dashed lines in the figure) elements with $D \ll 1$ are enriched much more markedly as the magma evolves, especially elements like Rb, K, U, Th where C_a/C_m^0 can be in the range 10–100. The rate of enrichment would become much faster for larger values of r. For example, consider the case of a tholeiitic basalt (K = 0.1%, Rb = 1 ppm) assimilating crustal rock with K = 3%, Rb = 100 ppm. If $r = 0.8$, at $F = 0.9$ the concentrations in the magma would have changed to K = 1.1% and Rb = 35 ppm, enrichments of 11 and 35 times. Other elements whose concentrations are similar in the initial magma and contaminant would show much smaller changes (less than a factor of 2). Small amounts of contamination could be an explanation of why K and Rb (and Ba?) show order of magnitude greater variations in some continental volcanic rocks than do many other elements including Sr and rare earths [14]. The sensitivity of K to contamination also demonstrates the danger in using K concentrations to infer mantle properties or determine depth to a magma source in continental regions [15].

For elements with $D > 1$ the assimilation-fractional crystallization (AFC) model differs from simple fractional crystallization mainly as F becomes small. For AFC a steady-state value is always reached, the value of which is given by equation (10). Consequently, for extensive fractionation these elements are not depleted in the magma indefinitely but reach a steady state value. Thus, for AFC (or for the magma recharge case discussed below) finite concentrations

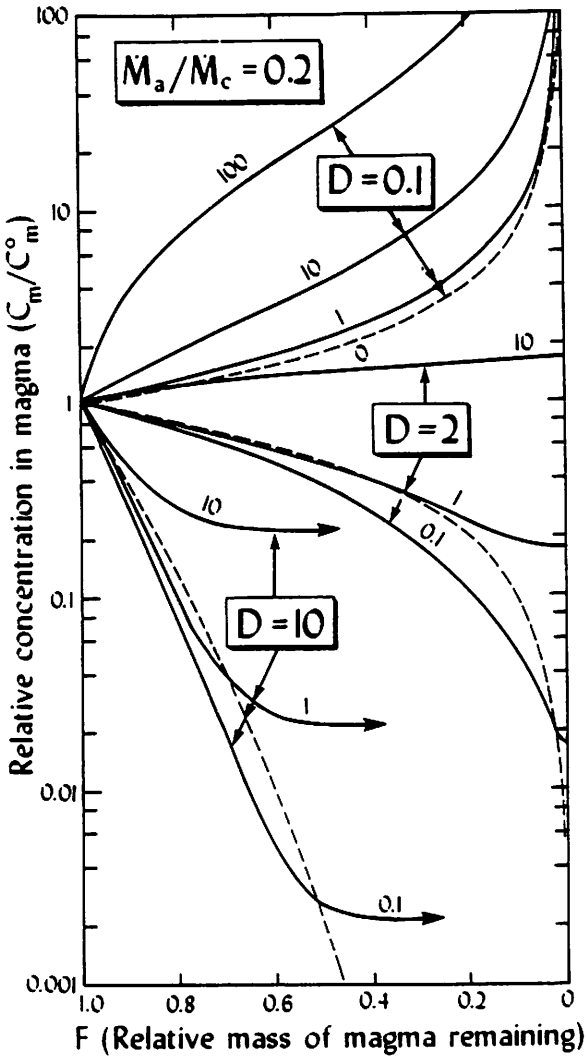

Fig. 2. Relationships between the relative concentration of an element in a magma experiencing assimilation-fractional crystallization (AFC) and the parameter F – the mass of the magma as a fraction of the original magma mass. The short-dashed lines are for simple fractional crystallization. The numbers on the curves give the values of C_a/C^0_m.

of compatible elements may not disallow the possibility of extensive fractionation as a means of enriching incompatible elements in a magma [6]. However, in actuality neither r nor D may necessarily remain constant with time so a steady-state concentration in a natural situation might never be reached. Also of note in Fig. 2 is that the effect on C_m of assimilation of material with various concentrations $C_a \leqslant C^0_m$ is almost independent of the concentration in the wallrock. The general criterion for an increasing concentration in the residual magma, from equation (4) is:

$$\frac{r}{r-1} C_a - zC_m < 0 \tag{11}$$

2.2. Isotopic ratios

For an isotopic ratio ϵ, the differential equation becomes:

$$\frac{d\epsilon_m}{dt} = r\frac{\dot{M}_c}{M_m}\frac{C_a}{C_m}(\epsilon_a - \epsilon_m) = \frac{\dot{M}_a}{M_m}\frac{C_a}{C_m}(\epsilon_a - \epsilon_m) \tag{12}$$

where ϵ_m = isotope ratio in the magma, and ϵ_a = isotope ratio in the wallrock.

This equation incorporates the assumption that the isotope ratio of the crystallizing phases is always the same as the magma. For the case $r = 1$, equation (12) can be integrated to give:

$$\begin{aligned}\epsilon_m = {} & \{(C_a/D)[1 - \exp(-DM_a/M_m)]\,\epsilon_a \\ & + C^0_m \exp(-DM_a/M_m)\,\epsilon^0_m\} \\ & \times \{(C_a/D)[1 - \exp(-DM_a/M_m)] \\ & + C^0_m \exp(-DM_a/M_m)\}^{-1}\end{aligned} \tag{13a}$$

where M is as defined above. This can also be written in the form:

$$\frac{\epsilon_m - \epsilon^0_m}{\epsilon_a - \epsilon^0_m} = 1 - (C^0_m/C_m)\exp(-DM_a/M_m) \tag{13b}$$

which gives the displacement in ϵ_m as a fraction of the total isotopic contrast $(\epsilon_a - \epsilon_m)$ between wallrock and initial magma. For the more general case of arbitrary, but constant $r \neq 1$ (12) can be written:

$$\frac{d\epsilon_m}{d\ln F} = \frac{r}{r-1}\frac{C_a}{C_m}(\epsilon_a - \epsilon_m) \tag{14}$$

where again t has been transformed to F using (5). This can be integrated to give:

$$\epsilon_m = \frac{\frac{r}{r-1}\frac{C_a}{z}(1 - F^{-z})\,\epsilon_a + C^0_m F^{-z}\epsilon^0_m}{\frac{r}{r-1}\frac{C_a}{z}(1 - F^{-z}) + C^0_m F^{-z}} \tag{15a}$$

where F and z are as previously defined. This can also be written:

$$\frac{\epsilon_m - \epsilon^0_m}{\epsilon_a - \epsilon^0_m} = 1 - (C^0_m/C_m)F^{-z} \tag{15b}$$

Depending on the system of interest ϵ could be replaced by any isotope ratio (e.g. $^{207}Pb/^{204}Pb$, $^{87}Sr/^{86}Sr$, $^{143}Nd/^{144}Nd$, $^{176}Hf/^{177}Hf$) or any normalized parameter describing such ratios (e.g. ϵ_{Sr}, ϵ_{Nd}).

For light stable isotopes there may be fractionation between the crystallizing phases and the magma so that the isotope ratio in the crystals is displaced from that in the magma by a factor α [16]. (This is also true for the radiogenic isotopes, but the effect is normalized away in the measurement procedure [17] and is of no concern here.) Since in most cases (e.g. oxygen, deuterium-hydrogen) normalized deviations from a standard ($\delta^{18}O$, δD) are used in lieu of the isotope ratios [17], it is equivalent to say that the δ value of the crystals is displaced from that of the magma by an amount $\Delta = \delta_{crystals} - \delta_{magma} \approx 1000 \ln \alpha$. In this case the differential equation becomes (ignoring terms of order 10^{-3}):

$$\frac{d\delta_m}{dt} = \frac{\dot{M}_c}{M_m}\left[r\frac{C_a}{C_m}(\delta_a - \delta_m) - D\Delta\right] \quad (16)$$

where δ_a and δ_m are the δ-values of the contaminant and magma respectively. This form is valid as long as $10^{-3}\Delta \ll 1$, which is true for oxygen in minerals crystallizing from a magma, but not necessarily for hydrogen [16].

For $r = 1$, this equation can be integrated to yield:

$$\delta_m - \delta_m^0 = \frac{C_a}{DC_m}(\delta_a - \delta_m^0 - \Delta) \times [1 - \exp(-DM_a/M_m)] - \frac{M_a}{M_m} D\Delta\left(1 - \frac{C_a}{DC_m}\right) \quad (17)$$

where C_m is given by equation (3). For $r \neq 1$, integration of (16) gives the general equation for crystallization-assimilation including isotopic fractionation:

$$\delta_m - \delta_m^0 = \left(\frac{r}{r-1}\right)\frac{C_a}{zC_m}\left[\delta_a - \delta_m^0 - \frac{D\Delta}{z(r-1)}\right] \times (1 - F^{-z}) - \frac{D\Delta}{r-1}\ln F\left[1 - \left(\frac{r}{r-1}\right)\frac{C_a}{zC_m}\right] \quad (18)$$

where F and z are as defined previously and C_m is given by equation (6). For a particular case of interest – that of oxygen isotopes – these equations can be considerably simplified if it is assumed that $D = 1$ and $C_a = C_m$, both reasonable approximations in most cases. With these approximations, equations (17) and (18) can be simplified to the following forms:

$$\delta_m - \delta_m^0 = (\delta_a - \delta_m^0 - \Delta)[1 - \exp(-M_a/M_m)] \quad (19)$$

for $r = 1$, and:

$$\delta_m - \delta_m^0 = (\delta_a - \delta_m^0 - \Delta/r)(1 - F^{-z}) \quad (20)$$

for $r \neq 1$, where in this case $z = r/(r-1)$. In general, $\delta_a - \delta_m^0$ can be in the range 0 to about 20 while Δ would rarely have an absolute value greater than one. The importance of mineral/melt fractionation relative to contamination should be small in most cases, but could become important for small r.

A limiting case of some interest for the interpretation of radiogenic isotope ratios is that for $D \ll 1$; in which case equation (13b) simplifies to:

$$\frac{\epsilon_m - \epsilon_m^0}{\epsilon_a - \epsilon_m^0} = (1 + C_m^0 M_m / C_a M_a)^{-1} \quad (21)$$

For this case even large amounts of assimilation may lead to small shifts in isotopic composition relative to the total shift possible. For $D \gg 1$, ϵ_m goes to ϵ_a as soon as M_a/M_m becomes large relative to D^{-1}, so small amounts of assimilation may cause very large isotopic shifts.

For the general model, when $D \ll 1$ and $r < 1$ the following limiting expression is obtained:

$$\lim_{F \to 0} \frac{\epsilon_m - \epsilon_m^0}{\epsilon_a - \epsilon_m^0}\left[1 - \left(\frac{r + D - 1}{r}\right)\frac{C_m^0}{C_a}\right]^{-1} \quad (22)$$

2.3. *Continuous recharge of a fractionating magma chamber*

The equations derived above are also applicable to a body of magma which is being recharged with fresh magma at the same time it is fractionally crystallizing (cf. [6]). If the newly added magma has the same composition as the original unfractionated magma, then C_a can be replaced by C_m^0, and $\dot{M}_r$ – the rate of recharge – can replace $\dot{M}_a$. For this case equations (3) and (6) become, respectively:

$$C_m/C_m^0 = \frac{1}{D}[1 - \exp(-DM_c/M_m)] + \exp(-DM_c/M_m) \quad (23)$$

$$C_m/C_m^0 = \frac{r}{(r-1)z}\,(1-F^{-z}) + F^{-z} \qquad (24)$$

where (23) applies to the case $\dot{M}_r = \dot{M}_c$ or ($r = 1$) and (24) applies otherwise. From (23) the steady state value, reached only if $M_c/M_m >> D^{-1}$, is simply:

$$C_m = C_m^0/D \qquad (25)$$

For the case $D << 1$ (23) reduces to: .

$$C_m/C_m^0 \approx 1 + M_c/M_m \qquad (26)$$

This equation clearly shows how an incompatible ($D << 1$) trace element can be enriched in a magma chamber, as has been emphasized by O'Hara as a possible explanation of incompatible-element-rich lavas erupted on oceanic islands [6]. Equations analogous to (9) and (10) can also be derived for $r \neq 1$. In Fig. 2, the curves shown for $C_a/C_m^0 = 1$ also apply to the recharge case. Equations (23) to (26) are written assuming the concentration of an element in the freshly added magma (C_r) is equal to C_m^0, but this is not required. The more general situation of $C_r \neq C_m^0$ is described fully by equations (3) and (6) to (11) by replacing C_a with C_r.

3. Discussion

The model and equations presented here may be applicable to a variety of situations where wallrock assimilation could be important. Under what circumstances, and to what extent, this process is important is still an unanswered question. Marsh and Kantha [18] have calculated that the ascent velocities of basaltic to andesitic magmas in the mantle may be large. Wallrock assimilation under such conditions might be minimal, especially since the wallrock, if it is peridotite, would be quite refractory.

However, Marsh and Kantha have also suggested that under certain conditions ascending magmas could induce melting in the mantle through which they pass. In such a case, the wallrock-derived partial melt could act as the contaminant. Depending upon conditions of pressure, temperature, water content, etc., such "assimilation" may or may not be accompanied by crystallization of the magma. Assimilation of a partial melt of the wallrock is completely described by the equations already presented (equations (3) and (6)) taking C_a to be the concentration of the element in the partial melt. C_a in this instance will depend upon the mineralogy of the wallrock, the concentration in the wallrock, and the fraction of melting [2]. For incipient melting $C_a = C_w/D'$ where C_w is the concentration in the wallrock and D' is the bulk solid/liquid distribution coefficient [2]. This model, which is analogous to the "wallrock reaction" proposed by Green and Ringwood [19] could aid in explaining the large enrichments of incompatible elements in some alkalic basalts. Note that this case is *not* the same as the zone melting equation given by Harris [12], which assumes complete melting of the wallrock and applies only to a constant magma mass.

In comparison to their ascent through the mantle, basic magmas probably experience a much slower, if not altogether aborted, ascent through silicic crustal rocks as a result of a greatly reduced density contrast, and hence a reduced buoyancy force. Even in the case of basalt magma rising through basaltic country rocks the density contrast would be much smaller than for basalt magma rising through peridotite. In these cases of slow or stalled magma ascent the wallrock, especially that above the magma chamber, may be significantly heated, and the magmas will cool if superheated or crystallize (and cool) if below the liquidus temperature [9]. Further magma ascent may in fact be prohibited unless or until the magma differentiates to a substantially less dense composition. The AFC model may be germaine in these instances [9].

3.1. Sr isotope and Rb, Sr concentration effects

For isotope ratios and associated elemental abundances the effects of AFC in comparison to simple mixing can be amply illustrated using conventional graphs of isotopic ratios versus elemental abundances and elemental ratios. Figs. 3 and 4 show such graphs for $^{87}Sr/^{86}Sr$, Sr abundance and Rb/Sr. Fig. 3a, b and c illustrate the differences generated by varying the values of the strontium distribution coefficient (D^{Sr}) and the parameter r. For all three cases the deviations from the simple mixing trajectory are profound. For r small the deviations are most pronounced, and the behavior approaches that expected for pure fractional crystallization. As r becomes larger the trajectories for all values of D^{Sr} collapse toward the simple mixing curve. For $r = 0.2$ (Fig. 3a) changes in the

$^{87}Sr/^{86}Sr$ of the magma are suppressed in comparison to changes in Sr concentration. If D^{Sr} is small, Sr in the magma increases rapidly with only small shifts in $^{87}Sr/^{86}Sr$. When D^{Sr} is in the range 0.7–1.0 the trajectory of the magma is very sensitive to the D^{Sr} value. When D^{Sr} is substantially greater than unity the Sr concentration again shifts rapidly in comparison to $^{87}Sr/^{86}Sr$. For this latter case the resultant curve mimics the shape of the simple mixing curve but does not extrapolate to the coordinates of the contaminant. Ignoring for the moment the effect of the parameter r, as a general rule, when fractional crystallization accompanies assimilation the properties of the contaminant can not be inferred unless the fractionating minerals and their proportions are known since they will control the value of D^{Sr}. Conversely, if the properties of the contaminant are known, the liquidus mineralogy can be inferred. D^{Sr}, for example, is mostly a function of the amount of plagioclase fractionation in comparison to mafic minerals (olivine, pyroxenes, amphibole) in basaltic systems. As r increases the shifts in Sr concentration are generally smaller for a given shift in $^{87}Sr/^{86}Sr$. It is clear, however, that there should be little reason to expect that magma contamination should follow simple mixing curves.

If the contaminant is not the bulk wallrock material, but instead is a partial melt of that wallrock, Fig. 3 can easily be used to infer the appropriate mixing trajectories. For example, if the partial melt of the wallrock had the same $^{87}Sr/^{86}Sr$, but a Sr concentration equal to half that of bulk wallrock, the effect would be to rotate all of the constant-D^{Sr} lines counterclockwise to a small extent.

In all probability as a magma moves through the continental crust r and D^{Sr} may be changing continuously. Consider a plausible history for a tholeiitic-type basaltic magma which enters the continental crust in an orogenic zone where ambient temperatures are already considerably elevated. Initially the wallrock may be at a temperature approaching that of the magma at a depth of 30–40 km. Heat loss by conduction would be minimal so the fusion heat of the wallrock could be approximately balanced by crystallization of an equal or only slightly larger mass of crystals (i.e. $r \lesssim 1$). Under these conditions D^{Sr} is also likely to be substantially less than one, since plagioclase is unlikely to be the major fractionating phase. This is because if the magma is dry, plagioclase density would be equal to or perhaps less than that of the magma [20] which would inhibit its fractionation relative to the denser pyroxenes and olivine. If the P_{H_2O} is substantial, then plagioclase saturation is suppressed [21]. As the magma moves up through the crust it will encounter cooler wallrocks and the heat budget of the system will work to inhibit assimilation, and accelerate crystallization; consequently, the value of r will decrease. Eventually, as differentiation proceeds, plagioclase will become the dominant fractionating phase [22] and D^{Sr} will increase. The Sr-$^{87}Sr/^{86}Sr$ path for such a magma is sketched in Fig. 3b. Note that if only the latter portion of this trend were sampled at the surface it would be very difficult to correctly deduce anything about either the magma source or the wallrock. The path associated with a similar magma traversing cooler (non-orogenic) crust is shown in Fig. 3a.

Mixing trajectories analogous to those of Fig. 3 are shown on a standard Sr evolution diagram in Fig. 4. For the purposes of the calculation the wallrock was arbitrarily assigned an Rb/Sr ratio of 0.5; the Sr concentration of the wallrock is the same as in Fig. 3. In addition to the mixing trajectories, Fig. 4 also gives Sr concentration contours for the $r = 1$ case, and a separate indication for the $r = 0.2$ case. The dashed curve (*a*) represents the hypothetical magma history discussed above and illustrated in Fig. 3b.

The mixing lines for constant D^{Sr} define gently curved lines which have slopes less than or equal to the slope of the straight line connecting the initial magma and the wallrock (≡ simple mixing curve) which is approximately the "model age" of the wallrock if Rb/Sr of the initial magma is near zero. Furthermore, the highest Sr concentrations are strictly associated with Rb/Sr-$^{87}Sr/^{86}Sr$ coordinates that lie close to the wallrock–initial magma line, with higher $^{87}Sr/^{86}Sr$ associated with *higher* Sr concentrations even though the wallrock has a very low Sr concentration.

3.2. Andean Cenozoic volcanism

James et al. [23] measured $^{87}Sr/^{86}Sr$ and Rb and Sr concentrations in some late Tertiary and Recent andesitic volcanics of the Andes in southern Peru.

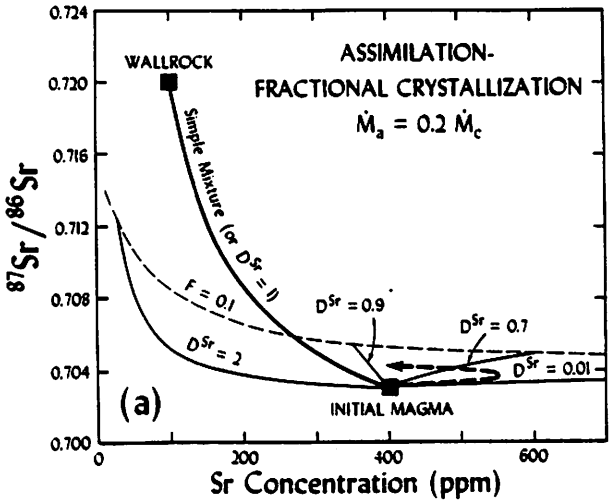

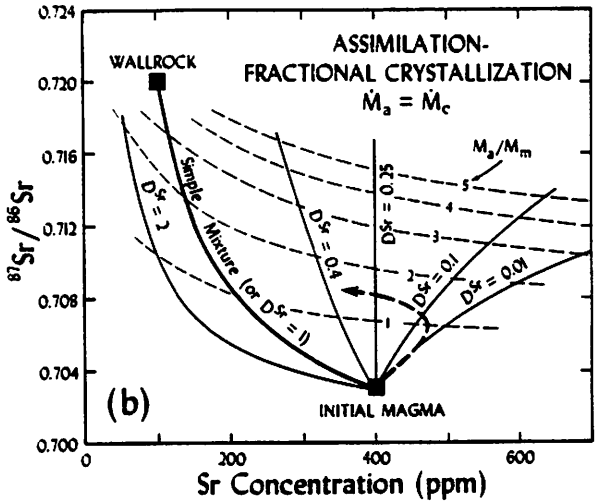

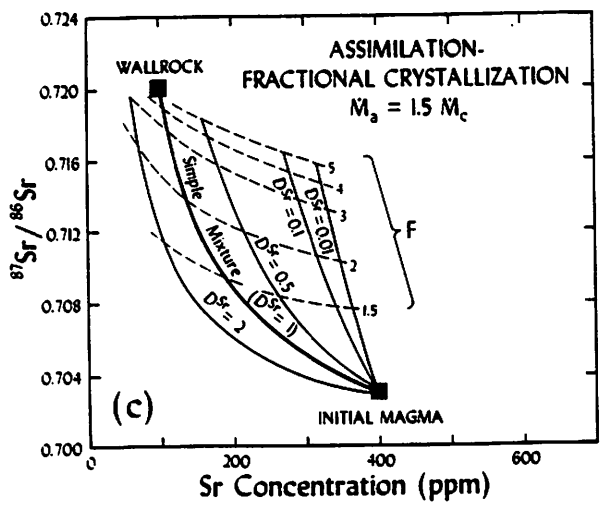

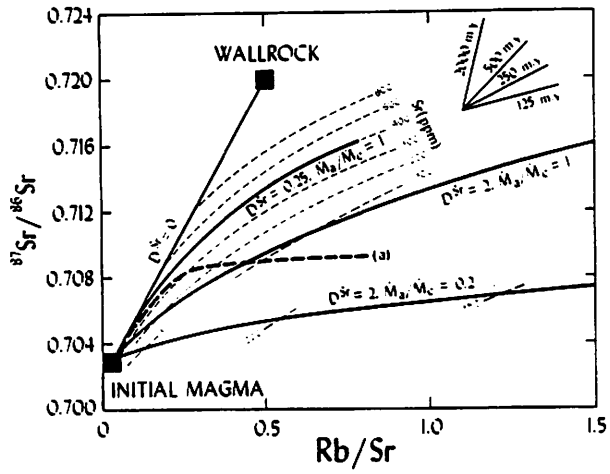

Fig. 4. $^{87}Sr/^{86}Sr$ and Rb/Sr shifts in a magma affected by assimilation and fractional crystallization. Trajectories are shown for $\dot{M}_a/\dot{M}_c = 1$ and different values of D^{Sr}, and for $\dot{M}_a/\dot{M}_c = 0.2$ for $D^{Sr} = 2$. For simplicity it was assumed that $D^{Rb} = 0$. Sr concentrations are contoured for the magma and wallrock concentrations given in Fig. 3. A notable feature of this graph is that increasing $^{87}Sr/^{86}Sr$ is associated with increasing Sr concentration (and low Rb/Sr) as long as D^{Sr} is small. The dashed curve labeled (*a*) represents a possible evolutionary path for a magma analogous to that shown in Fig. 3b. Linear arrays on this diagram are often assumed to have time significance. The relationship between slope and age is illustrated at upper right. This figure shows that quasi-linear arrays can be generated by the assimilation process, that the slopes of these arrays are controlled by physical parameters inherent in the model, and that the slopes may range from that of the simple mixture line (an approximation to the model age of the contaminant) to zero. Plagioclase-rich cumulate rocks could lie to the upper left of the simple mixture line ($D^{Sr} = 0$).

The rocks exhibited elevated $^{87}Sr/^{86}Sr$ ratios and the authors discussed whether these could have resulted from crustal contamination or instead had to be attributed to mantle magma sources. They concluded,

Fig. 3. $^{87}Sr/^{86}Sr$ and Sr concentration shifts in a magma affected by concurrent wallrock assimilation and fractional crystallization for different values of r ($= \dot{M}_a/\dot{M}_c$). D^{Sr} is the bulk distribution coefficient for Sr between the fractionating minerals and the magma. For basaltic systems D^{Sr} depends mostly on the amount of plagioclase fractionation relative to olivine, pyroxenes and amphibole. The heavy dashed lines on graphs (a) and (b) represent possible evolutionary paths as a magma body rises through the crust. These paths show the effects of decreasing r and increasing D^{Sr} as the magma evolves.

based solely on simple two-component mixing models, that the data could not be explained by crustal contamination, and therefore that old Rb-enriched mantle lithosphere underlay western South America. Furthermore, they argued that observed correlations between $^{87}Sr/^{86}Sr$ and Rb/Sr indicated meaningful ages of events in the subcontinental lithosphere. These "pseudoisochrons", along with others from additional localities were also used by Brooks et al. [24] to construct a general model for the evolution of subcontinental mantle.

The data of James et al. [23] are shown in Fig. 5. The number accompanying each point is the Sr concentration of that sample. The 2.7-AE isochron was calculated using an initial $^{87}Sr/^{86}Sr$ of 0.7012. The age of the basement under Peru is not known precisely, but indications are that it is older than 2 AE [23]. The general features of the Rb-Sr data are explicable in terms of an AFC model as can be seen by comparison with Fig. 4. In particular, the AFC model explains the high Sr concentrations, the restriction of high Sr concentrations to rocks with low Rb/Sr, and the tendency among the rocks with lowest Rb/Sr for higher Sr concentration in rocks with higher $^{87}Sr/^{86}Sr$ (i.e. the generally higher Sr concentrations of the Arequipa suite relative to the Barroso volcanics).

In the inset graph of Fig. 5 the data from the Arequipa volcanics are compared to the results of a specific AFC calculation, with the results displayed as in Fig. 4. The initial magma was assumed to have Sr = 400 ppm, Rb = 10 ppm and $^{87}Sr/^{86}Sr = 0.7030$. The contaminant was assumed to have Sr = 500 ppm, Rb = 40 ppm and $^{87}Sr/^{86}Sr = 0.71025$. These parameters for the contaminant are similar to those expected for a lower-crustal granulite terrain of ~2.7 AE age. It was further assumed that $r = 1$. The mixing trajectories for D^{Sr} values of 0, 0.25, 0.5 and 1.25 and the Sr concentration isopleths are shown on the inset graph. The model gives a good qualitative fit to most of the data. Considering the possible chemical and age variations in the contaminant, the tendency for r to decrease and D^{Sr} increase in the latter stages of magma evolution, it is clear that this contamination model can easily explain the data.

For the parameters chosen, the isotopic data require values of M_a/M_m of one or somewhat greater, indicating that the magmas, as they are erupted,

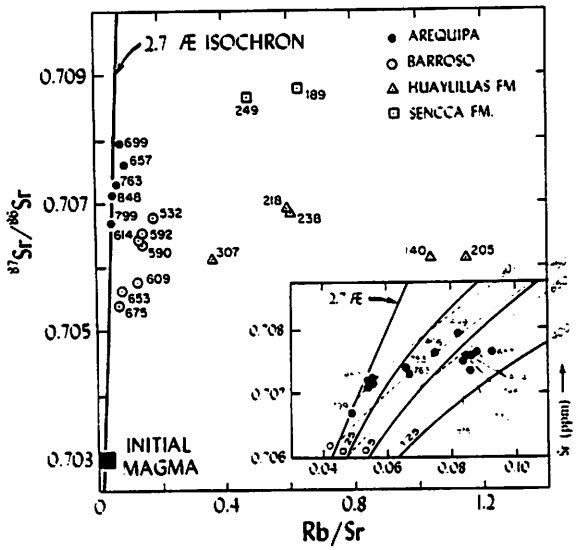

Fig. 5. Rb-Sr isotopic data from Andean Cenozoic volcanic rocks of Peru [23]. The numbers accompanying each point give the Sr concentration in ppm for that sample. The overall pattern of $^{87}Sr/^{86}Sr$, Rb/Sr and Sr concentration is close to that which would be expected for assimilation-fractional crystallization (Fig. 4) starting from an initial magma with isotopic characteristics similar to those of oceanic island arcs. Inset shows detail of Arequipa samples and the results of a model calculation described in the text.

represent about a 1 : 1 mix of mantle and crustal materials. The modeling also suggests that most of the contamination took place under conditions where plagioclase fractionation was minimal, probably near the base of the crust. To explain the Barroso data a change in parameters would be necessary. For instance, assuming the same characteristics for the initial magma and contaminant, a smaller value of r would be required.

The AFC model provides a fairly straightforward explanation of the Andean data, and thereby allows the geochemical, petrological and geophysical data for this region to be reconciled. Contamination, as might be expected in this region of thick crust, explains the isotopic data. The concurrent fractionation helps explain the trace element data, and the necessity for mantle-derived initial magmas can explain the Mesozoic-Cenozoic crustal thickening [23]. In addition, the model accounts for the "pseudoisochrons" [24], since correlations between $^{87}Sr/^{86}Sr$ and Rb/Sr are expected for this contamination model. As shown in Fig. 4 these correlations will

always give apparent "ages" that are less than the basement (contaminant) age. But these "ages" have no time significance and probably have nothing to do with the properties of the mantle. The model is also petrologically plausible, since assimilation of calc-alkaline crustal materials will not affect the basic major element chemistry of the magma series [9] except for an enrichment in K which is incompatible during fractionation. This could explain why these Andean lavas are generally somewhat richer in K (also other large-ion elements) than their oceanic counterparts [23,25]. Although this treatment does not prove that contamination was involved in the evolution of the Andean magmas, it demonstrates that there is nothing in the trace element and isotopic characteristics of the rocks that is incompatible with contamination having played a prominent role. Contamination of Andean lavas of this region is also suggested by Nd [26] and Pb [27] isotopic results. The AFC model also appears to readily fit data from the Sierra Nevada [28], another magmatic arc with similarities to the Andes.

3.3. Nd-Sr isotopic systematics

In general, more constraints on petrogenetic processes are provided when isotopic variations of two or more elements are considered. As further illustration of the isotopic patterns produced by the AFC model, mixing lines which could be generated for Nd and Sr isotopes are illustrated in Fig. 6 on a graph of ϵ_{Nd} versus ϵ_{Sr} (cf. DePaolo and Wasserburg [29] for explanation of notation). For the example shown, Sr and Nd are taken to have the same concentration in wallrock and initial magma. Simple mixtures of the wallrock and magma would have ϵ_{Sr}, ϵ_{Nd} compositions lying along a straight line connecting the two points. The AFC situation can result in widely varying isotopic effects depending on the relative size of D_{Nd} and D_{Sr} and $\dot{M}_a/\dot{M}_c$. If D_{Nd} and D_{Sr} are of similar magnitude, the curves obtained follow closely the simple mixing trajectory, but if the distribution coefficients differ markedly, especially if one is greater than – and the other less than – unity, the curves may depart drastically from the simple mixture curve. For many geologically plausible situations D_{Nd} will be small whereas D_{Sr} may be small or large

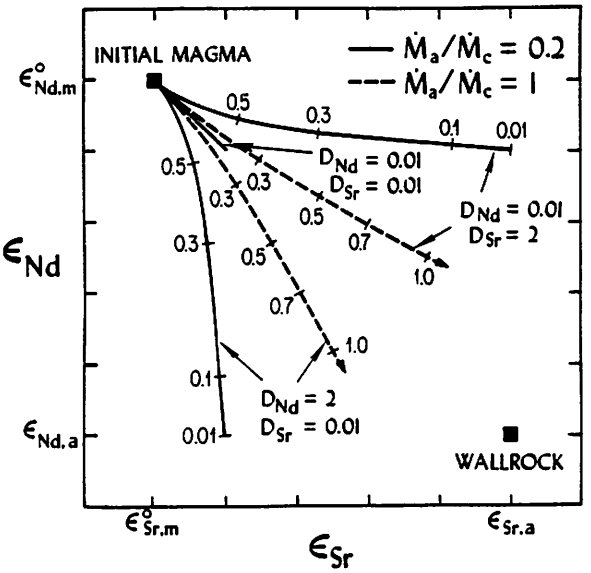

Fig. 6. ϵ_{Nd}-ϵ_{Sr} "mixing lines" for assimilation-fractional crystallization in a magma chamber. Square symbols represent the isotopic composition of initial magma and wallrock. $r = \dot{M}_a/\dot{M}_c$ is assumed constant in the calculation. Tick marks on the solid curves are labelled with the value of F, the relative amount of magma remaining. Ticks on the dashed curves give M_a/M_m. The curves were calculated for a case of equal Nd and Sr concentrations in wallrock and initial magma. Note that curves do not necessarily connect the endmembers (cf. [10]) and that when $D << 1$, the extent to which ϵ_m can be displaced is limited to a small fraction of the isotopic difference between the initial magma and the wallrock. The curve describing simple mixing for this example would be a straight line connecting the endmembers.

depending upon whether plagioclase is an important fractionating mineral. The case shown of large D_{Nd} and small D_{Sr} may be less common (cf. Irving [30] for a summary of distribution coefficients), but could apply if amphibole fractionation were important. These calculations clearly show that previous generalizations of isotopic effects caused by mixing [9,13, 31] may require some reevaluation. In particular, the curvature of mixing lines on this type of diagram is related to the relative value of Sr/Nd in the two endmembers for the simple mixture model. For AFC, however, curvature may be controlled to a large extent by other parameters.

The limitation on the displacement of the isotopic ratio in the magma when $D << 1$ is clearly illustrated in Fig. 6. For instance, for Nd isotopes, equation (22)

becomes:

$$\lim_{F\to 0} \frac{\epsilon_{Nd,m} - \epsilon^0_{Nd,m}}{\epsilon_{Nd,a} - \epsilon^0_{Nd,m}} = \left[1 + \left(\frac{r + D^{Nd} - 1}{r}\right)\frac{C^0_{Nd,m}}{C_{Nd,a}}\right]^{-1} \quad (27)$$

When the quantity in parentheses is >1 the total possible shift in $\epsilon_{Nd,m}$ can be much less than the isotopic difference ($\epsilon_{Nd,a} - \epsilon^0_{Nd,m}$) between initial magma and wallrock. This is shown by the solid curves in Fig. 6. For the uppermost curve shown, $D_{Nd} = 0.01$ and $C_{Nd,a}/C^0_{Nd,m} = 1$. With these values, the r.h.s. of equation (26) is just equal to r, which is 0.2 for this example. Within a suite of igneous rocks there could be a substantial variability in the amount of assimilation (for instance, variation of F from 0.5 to 0.1) but this variable assimilation would result in a restricted range of ϵ_{Nd} in comparison to the total difference in ϵ_{Nd} between the endmembers. For example, if $\epsilon^0_{Nd,m} = +10$ and $\epsilon_{Nd,a} = -20$, the portion of the upper curve between $F = 0.5$ and $F = 0.1$ spans only the range $\epsilon_{Nd,m} = +6$ to +4. This clustering of ϵ_{Nd} is just the opposite of what are usually assumed to be the consequences of mixing.

An important implication of this effect concerns the interpretation of isotopic data in continental volcanic rocks. DePaolo and Wasserburg [14] have noted that initial ϵ_{Nd} values of continental flood basalts cluster near $\epsilon_{Nd} = 0$. They argued that this clustering suggested that the observed ϵ_{Nd} did not represent a mixture between a mantle-derived magma with positive-ϵ_{Nd} and negative-ϵ_{Nd} continental crust. Equation (26), however, shows that clustering could result even if mixing due to crustal assimilation were involved. If the ϵ_{Nd} of the continental flood basalts could be explained by crustal assimilation, it would remove any necessity for a difference between suboceanic and subcontinental mantle, and could allow a wider range of plausible earth models [32]. This problem deserves further scrutiny but can only be addressed by considering petrologic, trace element, and regional geologic constraints in each case.

3.4. Crustal contamination vs. "enriched" reservoirs in the mantle?

An issue of recent concern is whether the fractionated trace element patterns and crust-like isotopic ratios of Nd and Sr in some basalts represent special "enriched" regions of the mantle or instead are simply the result of crustal assimilation (cf. [20]).

The arguments in favor of enriched mantle sources for these basalts have been based in large part upon trace element patterns which "require" a special chemical composition for the magma source [34]. Evidence for the existence of such regions of the mantle also comes from the Nd isotopic composition of the basalts, in particular negative values of ϵ_{Nd}, the normalized isotopic parameter which describes variations of $^{143}Nd/^{144}Nd$ [29].

Fig. 7 shows ϵ_{Nd} data for a variety of young igneous rocks emplaced into continental crust. The total range of ϵ_{Nd} values exhibited by rocks from a given region is shown by a vertical bar. The horizontal axis is the estimated age of the country rocks at the time the magmas were emplaced. The zone at the top

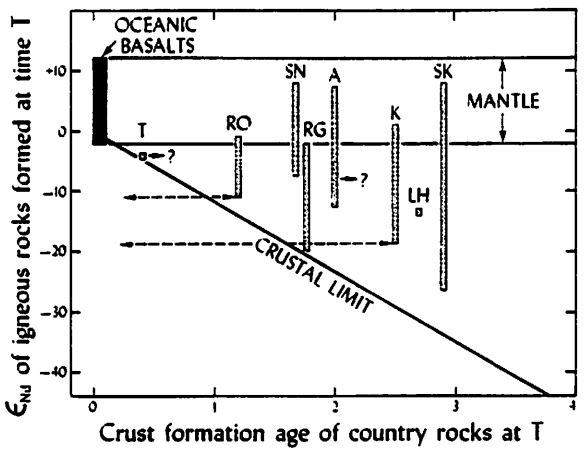

Fig. 7. Initial ϵ_{Nd} range of several rock suites plotted against the "age" of the country rocks at the time of emplacement/eruption. The ϵ_{Nd} zone labelled "Mantle" is the range of ϵ_{Nd} in the mantle as indicated by oceanic basalts [35]. The "crustal limit" represents the lowest value of ϵ_{Nd} which would be likely in crustal rocks of a given age [31]. Horizontal dashed arrows indicate the uncertainty in the country rock age. Age here means the time that the crustal material was formed from the mantle [36]. Symbols: T = Tasmanian dolerite [43], RO = Roccamonfina [33], SN = Sierra Nevada [44], RG = Rio Grande rift [45], A = Andes [26,46], K = Karroo basalts [29,26], LH = Leucite Hills [26], SK = Skye [47]. Points plotting below the crustal limit would support the existence of negative-ϵ_{Nd} mantle reservoirs. The existing data must be considered suggestive evidence that negative-ϵ_{Nd} igneous rocks result from crustal involvement in magma evolution.

represents the range of ϵ_{Nd} expected in various mantle reservoirs and is determined from oceanic basalts [35]. The diagonal line represents the lowest present-day ϵ_{Nd} expected in crustal rocks as a function of their age [31]. Thus, for example, if a basalt is emplaced into crust 2.0 AE old, the range of ϵ_{Nd} in the mantle and all available contaminating materials is from +12 down to −25. Fig. 7 shows that although in many cases the country rock "age" is poorly known there is a clear suggestion that negative ϵ_{Nd} values may be confined to regions where negative ϵ_{Nd} crust already was in existence.

Independent of any petrologic constraints, this is strong circumstantial evidence that crustal contamination (assimilation, anatexis) may be reponsible for perhaps all observed negative-ϵ_{Nd} igneous rocks. Clear evidence for enriched mantle would be provided by rocks that plotted distinctly below the diagonal line in Fig. 7. The Roccamonfina lavas could be such a case, but the "age" of the country rock is not yet known, in terms of the T_{DM} or crust-formation age [36]. Because the country rocks are largely sedimentary and metasedimentary, the T_{DM} are may be much greater than the geologic age. The igneous rocks of Kerguelen have recently been cited as another possible indicator of enriched mantle [37], but the continent-like geophysical structure of the Kerguelen Ridge and its predrift juxtaposition with very old continental crustal regions [38] makes this a highly dubious inference. The circumstantial evidence for crustal involvement in the generation of negative-ϵ_{Nd} igneous rocks is substantial. The models discussed in this paper suggest that zeroeth-order models for trace element patterns such as simple mixing are insufficient to rule out this possibility, as evidenced by the Andean data discussed above. In general, it is necessary to entertain a broader class of contamination mechanisms in order to argue strongly against the possibility of contamination. However, alternative explanations do exist which could be compatible with relationships shown in Fig. 7. For instance, *old* "enriched mantle" may exist only beneath old continental crust. Perhaps it represents a sub-Moho "lower crust" in terms of its geochemical properties as is suggested by some trace element and isotopic data on ultramafic nodules [39]. The apparent correlation seen in Fig. 7 between crustal age and the lower limit ϵ_{Nd} observed, would suggest that this (hypothetical) subcontinental enriched mantle in each case has a maximum age roughly equal to that of the overlying crust. The lack of any substantive isotopic evidence that old enriched mantle exists in oceanic regions suggests that the bulk of the upper mantle is mixed on a sufficiently rapid time scale that any such chemically unusual reservoirs are not preserved for time periods greater than 0.2–0.4 AE [40]. The restriction of any old enriched mantle reservoirs to the subcontinental lithosphere has not been recognized in some recently proposed models of mantle evolution [41], which has led to improbable models for their origin. Furthermore, although there are data that suggest the existence of enriched mantle, there is as yet no way to determine if a volumetrically significant fraction of the subcontinental mantle has such properties.

4. Conclusions

The equations given above provide the means for easily modeling the effects of coupled wallrock assimilation and fractional crystallization. When the compositions of the endmembers are known or can be estimated, this mixing/differentiation model may allow trace element and isotopic data to be used to place constraints on the rates and extent of assimilation and the liquidus phases involved. In general, the amount of assimilation will depend upon physical parameters (temperature contrast between magma and wallrock, rate of magma ascent, fusion temperature of wallrock and magma) as will the amount of fractional crystallization (magma rheology, density contrast between crystals and liquid). The differential equations given here have been expressed in a form which emphasizes time dependence and magma mass to allow the assimilation and crystallization rates to be related to heat flow, buoyancy and crystallization time scales in situations where that might be possible. The choice of magma mass (F) as the independent variable for the equations given was arbitrary, and necessitated the artificial distinction between models involving constant versus changing magma mass. Alternatively, a single set of equations could be derived with the mass of assimilated material (M_a) as the dependent variable. The approach represented by equation (1) is quite general and could be extended to describe magma chamber venting as well as frac-

tional crystallization, wallrock assimilation and magma recharge. Closed-form solutions cannot be obtained if all four transport phenomena are considered simultaneously (except in very specialized cases), but the equations could be solved numerically if a sufficient number of parameters are specified.

Taylor [10] has calculated that assimilation of 1 g of wallrock initially at 150°C into a magma at 1150°C could be thermally balanced by crystallization of 3.25 g of crystals. He estimated an upper limit value of r, therefore, to be about 0.3 ($\approx 1/3.25$). Heat loss by conduction at the margins of the magma chamber would tend to decrease r. This calculation, however, is for cold country rock. An analogous calculation for country rock at 1000°C (lower crust in regions of active volcanism and high heat flow?), would result in an upper limit r of about 1. Furthermore, it is possible that due to convection in the magma chamber and/or increasing viscosity caused by crystallization [29] and SiO_2-enrichment, that crystallizing phases may not separate from a highly siliceous magma. In this case the value of r may be larger because the latent heat is still available, but fractional crystallization is suppressed. For the model to remain applicable for this crystal mush the crystals must retain equilibrium with the residual melt. If this were not the case then intercrystalline isotopic and trace element inhomogeneity would be observed in the product rock. As $r \to \infty$ the simple mixing case is recovered. *Clearly, when the simple mixing model for assimilation – which is equivalent to no fractional crystallization – is viewed as a special case of the more general model discussed here, the unlikelihood of its applicability becomes apparent* [9].

Recognition of the model dependence of inferences from trace element patterns, and the need for higher-order models, will be critical for the reconcilement of trace elements with petrologic and isotopic inferences. As discussed above, a process may appear to be incompatible with a particular data set when its trace element signature is modelled in the simplest way, but a variant of that process may be in fact quite plausible in the context of more sophisticated models. A small number of examples have been discussed here, but it appears that the approach used may have wide applicability. It represents a step toward a broader understanding of trace element and isotopic variations in igneous rocks, but more sophisticated models may be necessary to fully appreciate these data and to glean from them their full yield of petrogenetic information.

Acknowledgements

Comments on an earlier version of this manuscript by L. Raedeke, and reviews by R. Gregory, R. Hill, and an anonymous reviewer were of considerable aid. This work has been supported by NSF grant EAR 78-12966.

References

1 P.W. Gast, Trace element fractionation and the origin of tholeiitic and alkaline magma types, Geochim. Cosmochim. Acta 32 (1968) 1057.
2 D.M. Shaw, Trace element fractionation during anatexis, Geochim. Cosmochim. Acta 40 (1970) 73.
3 R.W. Kay and P.W. Gast, The rare earth content and origin of alkali-rich basalts, J. Geol. 81 (1973) 653.
4 F.A. Frey, D.H. Green and S.D. Roy, Integrated models of basalt petrogenesis: a study of quartz tholeiites to olivine melilitites from south eastern Australia utilizing geochemical and experimental petrological data, J. Petrol. 19 (1978) 463.
5 I.S.E. Carmichael, J. Nicholls, F.J. Spera, B.J. Wood and S.A. Nelson, High-temperature properties of silicate liquids: applications to the equilibration and ascent of basic magma, Philos. Trans. R. Soc. London, Ser. A, 286 (1977) 373.
6 M.J. O'Hara, Geochemical evolution during fractional crystallization of a periodically refilled magma chamber, Nature 266 (1977) 503.
7 C.H. Langmuir, J.F. Bender, A.E. Bence, G.N. Hanson and S.R. Taylor, Petrogenesis of basalts from the FAMOUS area: Mid-Atlantic Ridge, Earth Planet. Sci. Lett. 36 (1977) 133.
8 C.J. Allègre and J.F. Minster, Quantitative models of trace element behavior in magmatic processes, Earth Planet. Sci. Lett. 38 (1978) 1.
9 N.L. Bowen, The Evolution of the Igneous Rocks (Dover, New York, N.Y., 1928) 332 pp.
10 H.P. Taylor, Jr., The effects of assimilation of country rocks by magmas on $^{18}O/^{16}O$ and $^{87}Sr/^{86}Sr$ systematics in igneous rocks, Earth Planet. Sci. Lett. 47 (1980) 243.
11 F. Barker, D.R. Wones, W.N. Sharpe and G.A. Desborough, The Pikes Peak Batholith, Colorado Front Range, and a model for the origin of the gabbro-anorthosite-syenite-potassic granite suite, Precambrian Res. 2 (1975) 97.
12 P.G. Harris, Origin of alkaline magmas as a result of anatexis, in: The Alkaline Rocks, H. Sorensen, ed. (Wiley, New York, N.Y., 1974) 427.

13 R. Vollmer, Rb-Sr and U-Th-Pb systematics of alkaline rocks: the alkaline rocks from Italy, Geochim. Cosmochim. Acta 40 (1976) 283.
14 D.J. DePaolo and G.J. Wasserburg, Neodymium isotopes in flood basalts from the Siberian Platform and inferences about their mantle sources, Proc. Natl. Acad. Sci. U.S.A. 76 (1979) 3056.
15 P.W. Lipman, H.J. Prostka and R.L. Christiansen, Evolving subduction zones in the Western United States, as interpreted from igneous rocks, Science 174 (1971) 821.
16 H.P. Taylor and S. Epstein, Relationship between $^{18}O/^{16}O$ ratios in coexisting minerals of igneous and metamorphic rocks, 2. Application to petrologic problems, Geol. Soc. Am. Bull. 73 (1962) 675.
17 G. Faure, Principles of Isotope Geology (Wiley, Santa Barbara, Calif., 1977) 464 pp.
18 B.D. Marsh and L.H. Kantha, On the heat and mass transfer from an ascending magma, Earth Planet. Sci. Lett. 39 (1978) 435–443.
19 D.H. Green and A.E. Ringwood, The genesis of basaltic magmas, Contrib. Mineral. Petrol. 15 (1967) 103.
20 I. Kushiro, Viscosity, density, and structure of silicate melts at high pressures, and their petrological applications, in: Physics of Magmatic Processes, R.B. Hargraves, ed. (Princeton University Press, Princeton, N.J., 1980) 93.
21 H.S. Yoder and C.E. Tilley, Origin of basalt magmas: an experimental study of natural and synthetic rock systems, J. Petrol. 3 (1962) 342.
22 P.J. Wyllie, Magmas and volatile components, Am. Mineral. 64 (1979) 469.
23 D.E. James, C. Brooks and A. Cuyubamba, Andean Cenozoic volcanism: magma genesis in the light of strontium isotopic composition and trace element geochemistry, Geol. Soc. Am. Bull. 87 (1976) 592.
24 C. Brooks, D.E. James and S.R. Hart, Ancient lithosphere: its role in young continental volcanism, Science 193 (1976) 1086.
25 R.W. Johnson, Distribution and major element chemistry of late Cenozoic volcanoes at the southern margin of the Bismarck Sea, Papua, New Guinea, Bur. Miner. Resour. Aust. Rep. 188 (1977).
26 D.J. DePaolo and G.J. Wasserburg, The sources of island arcs as indicated by Nd and Sr isotopic studies, Geophys. Res. Lett. 4 (1977) 465.
27 G.R. Tilton and B.A. Barreiro, Origin of lead in Andean calc-alkaline lavas, southern Peru, Science 210 (1980) 1245.
28 R.W. Kistler and Z.E. Peterman, Variations in Sr, Rb, K, Na and initial $^{87}Sr/^{86}Sr$ in Mesozoic granitic rocks and intruded wall rocks in Central California, Geol. Soc. Am. Bull. 84 (1973) 3489.
29 D.J. DePaolo and G.J. Wasserburg, Nd isotopic variations and petrogenetic models, Geophys. Res. Lett. 3 (1976) 249.
30 A.J. Irving, A review of experimental studies of crystal/liquid partitioning, Geochim. Cosmochim. Acta 42 (1978) 743.
31 D.J. DePaolo and G.J. Wasserburg, Petrogenetic mixing models and Nd-Sr isotopic patterns, Geochim. Cosmochim. Acta 43 (1979) 615.
32 G.J. Wasserburg and D.J. DePaolo, Models of earth structure inferred from neodymium and strontium isotopic abundances, Proc. Natl. Acad. Sci. U.S.A. 76 (1979) 3594.
33 S.R. Carter, N.M. Evensen, P.J. Hamilton and R.K. O'Nions, Continental volcanics derived from enriched and depleted source regions: Nd- and Sr-isotope evidence, Earth Planet. Sci. Lett. 37 (1978) 401.
34 S.S. Sun and G.N. Hanson, Origin of Ross Island basanitoids and limitations upon the heterogeneity of mantle sources for alkali basalts and nephelinites, Contrib. Mineral. Petrol. 52 (1975) 77.
35 R.K. O'Nions, P.J. Hamilton and N.M. Evensen, Variations in $^{143}Nd/^{144}Nd$ and $^{87}Sr/^{86}Sr$ ratios in oceanic basalts, Earth Planet. Sci. Lett. 34 (1977) 13.
36 D.J. DePaolo, Neodymium isotopes in the Colorado Front Range and implications for crust formation and mantle evolution in the Proterozoic, Nature (in press).
37 L. Dosso and V.R. Murthy, A Nd isotopic study of the Kerguelen Islands: inferences on enriched oceanic mantle sources, Earth Planet. Sci. Lett 48 (1980) 268.
38 D. MacKenzie and J.G. Sclater, The evolution of the Indian Ocean since the late Cretaceous, Geophys. J. R. Astron. Soc. 25 (1971) 437.
39 M. Menzies and V.R. Murthy, Enriched mantle: Nd and Sr isotopes in diopsides from kimberlite nodules, Nature 283 (1980) 634.
40 D.J. DePaolo and G.J. Wasserburg, Inferences about magma sources and mantle structure from variations of $^{143}Nd/^{144}Nd$, Geophys. Res. Lett. 3 (1976) 743.
41 D.L. Anderson, Early evolution of the mantle, Episodes 3 (1980) 3.
42 H.R. Shaw, Comments on viscosity, crystal settling and convection in granitic magmas, Am. J. Sci. 263 (1965) 120.
43 D.J. DePaolo, Nd and Sr isotope systematics of young continental igneous rocks, in: Short Papers of the Fourth International Conference, Geochronology, Cosmochronology, Isotope Geology, U.S. Geol. Surv. Open-File Rep. 78-701 (1978) 476 pp.
44 D.J. DePaolo, The sources of continental crust: Nd isotope evidence from the Sierra Nevada and Peninsular Ranges, Science 209 (1980) 684.
45 S. Williams and V.R. Murthy, Sources and genetic relationships of volcanic rocks from the northern Rio Grande rift: Rb-Sr and Sm-Nd evidence, EOS, Trans. Am. Geophys. Union 60 (1979) 407.
46 C.J. Hawkesworth, M.J. Norry, J.C. Roddick and P.E. Baker, $^{143}Nd/^{144}Nd$, $^{87}Sr/^{86}Sr$ and incompatible element variations in calc-alkaline andesites and plateau lavas from South America, Earth Planet. Sci. Lett. 42 (1979) 45.
47 S.R. Carter, N.M. Evensen, P.J. Hamilton and R.K. O'Nions, Neodymium and strontium evidence for crustal contamination of continental volcanics, Science 202 (1978) 743.